2-D ECE imaging diagnostic for comparative study of MHD instabilities in WEST tokamak

Y. B. Nam[1], R. Sabot[1], D. Elbeze[1], M. Kim[2], M. Choi[3], H. K. Park[2, 3], G. S. Yun[4], W. Lee[3], P. Lotte[1] and WEST team[1]

[1] *CEA, IRFM, Saint-Paul-lez-Durance, France*

[2] *Ulsan National Institute of Science and Technology, Ulsan, Korea*

[3] *National Fusion Research Institute, Daejeon, Korea*

[4] *Pohang University of Science and Technology, Pohang, Korea*

Introduction

WEST (W Environment for Steady state Tokamak) [1] is an upgrade of Tore Supra to study physics and technology of the first wall interaction for ITER (International Thermonuclear Experimental Reactor), with implementation of an actively cooled tungsten divertor. In order to reach the goal of long stable discharges with the new environment, detail characterization and comprehensive understanding of magnetohydrodynamic (MHD) instabilities and impurity transport are necessary.

Electron cyclotron emission (ECE) imaging [2,3,4] system is a microwave imaging diagnostic capable of measuring 2- or 3-dimensional distribution of the electron temperature (T_e) fluctuation in the plasma. ECE imaging has been proven to be a powerful tool for understanding MHD and turbulence phenomena, by visualizing spatial and temporal evolution of T_e fluctuation for direct comparison with theories and simulations.

2-D ECE imaging diagnostic system for WEST [5] has been developed under WEST-UNIST collaboration. The system fabrication is completed and ready for the first measurement of the background noise at the end of 2018. A tight available space in front of maintenance access port and indirect view to the plasma led to a unique design of vertically aligned diagnostic system, along with two mirrors inside the vacuum vessel. Laboratory test of the integrated imaging optics successfully demonstrated the focusing ability of the optical system.

Detection characteristics

Like other ECE imaging systems, the WEST ECE system is equivalent to a vertical stack of 24 1-D ECE radiometers. The ECE radiations collected by a detector is subdivided into 8 frequency ranges (i.e. equivalent to 8 radial channels with 0.6 GHz bandwidth and 0.9 GHz separation. 2-D images of T_e fluctuation are constructed based on simultaneously processed

$24 \times 8 = 192$ detection signals (24 vertical x 8 radial) for every 2 μs during 10 s of total measurement duration. Note that the 10 s can be divided and distributed to the targeted time ranges in a single experiment. The target radial detection range in the plasma can be selected from any radial location by controlling the large aperture imaging optics and the LO frequencies. The image size can be ~40 cm (vertical) × 8 ~ 15 cm (radial), depending on the target radial measurement location. The frequency range of the detection system is from 85 GHz to 130 GHz and this frequency range is equivalent to the O1 mode [6] at $B_t = 3.7\ T$.

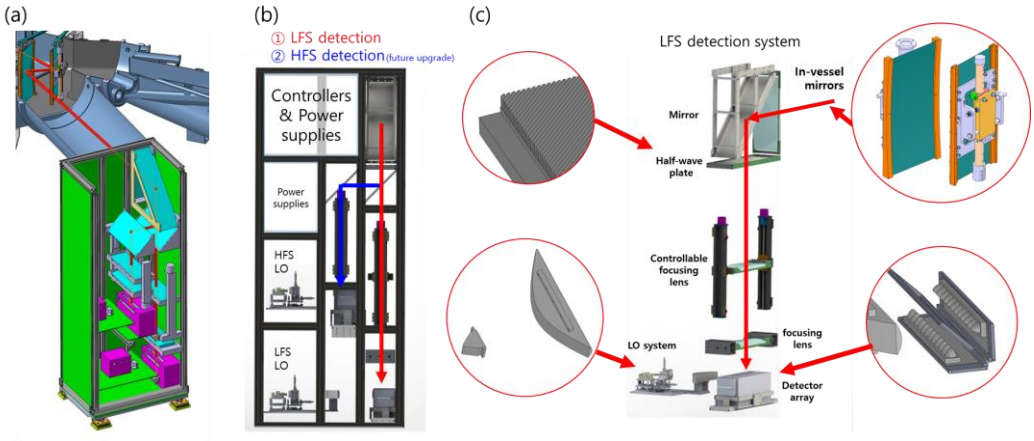

Fig. 1. (a) Schematic view of the optical enclosure and in-vessel mirrors installed in front of the man access port. The red lines represent the ECE beam path. **(b)** Side view of the interior structure of optical enclosure. **(c)** Detail elements of LFS detection system.

System components

The West ECE imaging diagnostic [5] system consists of an optical enclosure, in-vessel mirrors, and cubicles. The optical enclosure, housing the vertically aligned optical elements and a detector box, will be installed in front of the maintenance access port as shown in Fig. 1(a). Two concave mirrors will be installed inside the vacuum vessel to focus and redirect the ECE radiation to the optical enclosure entrance. The optical enclosure and the mirrors are designed to be easily removed with the crane and installed on the guiding rails whenever the maintenance access to the port is active. Cubicles will be put into the underground level to install the video modules and data acquisition boards. The diagnostic system will initially have a detection system optimized for the low field side (LFS) measurement as in Fig. 1(b). An additional system will be installed in the future for high field side (HFS) measurement.

Fig. 1(c) shows the optical elements comprising the LFS detection system. A half-wave plate [7] is utilized to change the polarization of the O-mode emission to be measured by the detection system designed for the X-mode beams. A focusing lens is mounted on the motor-driven guides for remote control. The 24 vertical detection channels are covered by

elliptical mini lenses [3] to maximize the channel responses. Two aspheric-lens LO optics [8] are specially designed for compactness and optimum LO coupling efficiency.

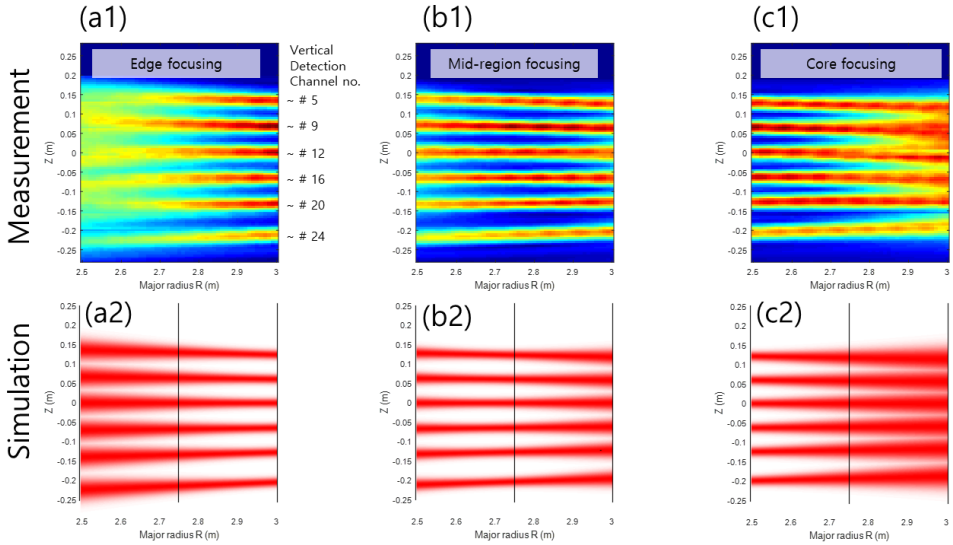

Fig. 2. Beam patterns showing the focus, size and location formed on plasma by the imaging optics. The focus of the image is set to LFS edge (a1), mid-region (b1), and core (c1) by controlling the focusing lens. The image from the numerical simulation, each focused on the LFS edge (a2), mid-region (b2), and core (c2) agrees well with the measurement.

Laboratory characterization of the imaging optics

The optical properties of the integrated imaging optics have been characterized in the laboratory. The laboratory characterization is performed in reversed beam path: A microwave Gaussian beam source is placed at the position of the detection channel, and the corresponding vertical and horizontal beam patterns at the plasma position are measured. Note that the elliptical mini lens in front of the detection channel modifies the angular response similar to that of the Gaussian beam perpendicularly impinging on the detector. The beam path has been simplified by removing a flat mirror and adjusting the angle of the in-vessel mirrors, which have negligible effect on the beam pattern.

Fig. 2 (a1), (b1), (c1) shows the composite images of the vertical beam patterns formed by 6 different vertical channels, depending on the focusing lens setup. The result shows that the imaging optics can freely focus on any radial location on LFS of the plasma($R = 2.5 \sim 3$ m). Note that the vertical zoom at the focus is almost invariant (~1.4 magnification) and the vertical coverage is kept at ~ 40 cm. Since the 8 ~ 15 cm radial coverage is well within the Rayleigh range (~30 cm), images provided by the WEST ECEI will be clearly focused on all 8 radial channels, almost independent of the focusing lens setup. Fig. (a2), (b2), (c2) shows the images from the numerical simulations, which agree perfectly with the measurements.

Conclusion and future works

An ECE imaging diagnostic has been developed under UNIST-WEST Collaboration, and the first background measurement is anticipated in the end of 2018. WEST ECEI diagnostic can provide 2-D T_e fluctuation images of the MHD instabilities. The spatial coverage is 40 cm (vertical) × 8~15 cm (horizontal) region with 24×8=192 pixels in the plasma and time resolutions is 2 μs.

The plasma facing reflective optics will be installed inside the vacuum vessel, and the rest of the imaging optics and detection system will be installed inside the vertically aligned optical enclosure. Laboratory characterization of imaging optics demonstrated that the imaging optics can freely focus on any radial position in LFS while providing clear images at all radial positions to be covered.

2-D ECE images with high temporal and spatial resolution enable to study the detail structure of the MHD instabilities. Thus, direct comparative study of the images with that of MHD simulations and/or other diagnostic devices will provide a comprehensive understanding of the underlying physics. For better understanding of the measurement, a synthetic image reconstruction tool for XTOR code is on development for numerical validation. The tool will provide synthetic images from XTOR result, taking into account the spatial resolution, instrumental effect and broadening effect of the ECEI system. The WEST ECE images will also be cross-compared with the 2-D reconstructed images of electron density obtained from 1-D reflectometry on WEST [9] to understand the simultaneous evolution of the temperature and density fluctuations. Comparative studies with KSTAR ECE images will provide the effect of the tungsten impurities on the instabilities.

*Work supported by a grant from the Région Sud Provence-Alpes-Côte d'Azur of France (DEB 1501376) and by the NRF of Korea (NRF- 2014 M1A 7A1A03029865).

References

[1]J. Bucalossi *et al*., Fusion eng. Des. Instrum. **86**, 684 (2011).

[2]G. S. Yun *et al*., Rev. Sci. Instrum. **85**, 11D820 (2014).

[3]B. Tobias *et al*., Rev. Sci. Instrum. **81**, 10D928 (2010).

[4]I. G. J. Classen *et al*, Rev. Sci. Instrum. **81**, 10D929 (2010).

[5]Y. Nam *et al*, Rev. Sci. Instrum. **87**, 11E135 (2016).

[6]M. Bornatici *et al*., Nucl. Fusion **23**, 1153 (1983).

[7]J. Lee *et al*., J. Instrum. **7**, C01037 (2012).

[8]Y. Nam *et al*, Rev. Sci. Instrum. **87**, 11E130 (2016).

[9]R. Sabot *et al*, Comptes rendus de physicque **17**, 1018-1026 (2016).